Shear heating-induced thermal pressurization during earthquake nucleation

Stuart V. Schmitt — Department of Geophysics, Stanford University — schmitt@stanford.edu
Paul Segall — Department of Geophysics, Stanford University
Takanori Matsuzawa — National Research Institute for Earth Science and Disaster Prevention, Japan

1. INTRODUCTION

Prompted by the absence of large heat flow anomalies near faults and the global paucity of friction-melt pseudotachylite, many researchers have considered the role of pore fluids as a dynamic weakening mechanism during earthquake rupture. The hypothesis is that shear heating pressurizes the pore fluid faster than it can diffuse away, thereby reducing the effective stress on the fault. Concurrently, the development of rate- and state-dependent friction theories has provided compelling models of how earthquakes nucleate from "locked" faults. The geophysical community has largely considered thermal pressurization in the context of large earthquakes and the rate- and state-dependent friction in the context of earthquake initiation. Yet recent studies [for example, *Ide & Beroza*, 2001] have shown that stress drop does not correlate with earthquake magnitude for events as small as $M_w = -3.5$. The implication is that there is no onset of a different fault weakening mechanism at any time during slip at seismic speeds.

Segall & Rice [2006] suggested that thermal effects may become dominant during the quasi-static nucleation phase, well before the onset of seismic radiation. Using the slip evolution given by rate- and state-dependent friction—along with reasonable estimates of heat and pore pressure transport parameters—they estimated that thermal pressurization dominates weakening at slip rates in excess of 10^{-5} to 10^{-3} m/s.

We present the results of numerical simulations that indicate that thermal pressurization is indeed the dominant fault weakening mechanism at speeds near 10^{-4} m/s—speeds encountered during nucleation. Our simulations fully couple friction, elasticity, seismic radiation, and fluid transport.

2. DESCRIPTION OF MODEL

- 2D finite difference diffusion grid.
- Shear heating is a boundary condition.
- Diffusion away from fault only.
- Grid refinement as accuracy demands.
- Stress rate and slip rate related through a Hilbert transform in the Fourier domain.
- Driven at "plate velocity" at the edges.
- Started with a slightly higher velocity in the middle to control site of nucleation.

Figure 1. Schematic of model

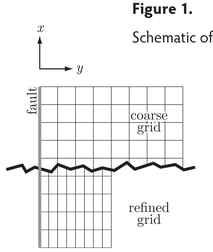

3. GOVERNING EQUATIONS

A. Shear stress on the fault

Elastic stress interaction:

$$\tau_{el}(x) = -\frac{G}{2\pi}\int_{-\infty}^{\infty}\frac{1}{x-\xi}\frac{\partial u}{\partial \xi}\,d\xi\,. \qquad (1)$$

Seismic radiation—radiation damping approximation [*Rice*, 1993]:

$$\tau_{rad} = \frac{G}{2v_s}v\,. \qquad (2)$$

Rate- and state-dependent friction:

$$\tau_{fric} = \left[\mu_0 + a\ln\frac{v}{v_0} + b\ln\frac{\theta v_0}{d_c}\right]\sigma_{eff}\,, \qquad (3)$$

with

$$\frac{d\theta}{dt} = 1 - \frac{\theta v}{d_c}\,, \quad \text{the "aging" law, and}$$

$$\frac{d\theta}{dt} = -\frac{\theta v}{d_c}\ln\frac{\theta v}{d_c}\,, \quad \text{the "slip" law.}$$

Together, eqs. (1)–(3) form the equation of motion

$$-\frac{G}{2\pi}\int_{-\infty}^{\infty}\frac{1}{x-\xi}\frac{\partial u}{\partial \xi}\,d\xi - \left[\mu_0 + a\ln\frac{v}{v_0} + b\ln\frac{\theta v_0}{d_c}\right][\sigma - p(t)] - \frac{G}{2v_s}v = 0\,. \qquad (4)$$

Table of parameters

G	shear modulus	10 GPa
v_s	s-wave velocity	3700 m/s
μ_0	nominal friction	0.6
a	friction velocity effect	0.015
b	friction state effect	0.019
d_c	slip weakening distance	100 μm
h	shear zone thickness	100 μm
c_{th}	thermal diffusivity	10^{-6} m²/s
c_{hyd}	hydraulic diffusivity	10^{-6} m²/s
ρc_v	density × heat capacity	2.86 MPa/K
Λ	thermal coupling param.	0.8 MPa/K
θ	frictional state	
γ	shear strain	
v	slip speed	
q_h	heat flux	
T	temperature (change)	
p	pore pressure (change)	
λ_f	pore fluid expansivity	
λ_ϕ	pore expansivity	
β_f	pore fluid compressibility	
β_ϕ	pore compressibility	

B. Generation and transport of fluid and heat

Energy balance for heat generation and transport:

$$\tau_{el}\frac{d\gamma}{dt} - k_{th}\frac{\partial q_h}{\partial y} = \rho c_v\frac{\partial T}{\partial t}\,. \qquad (5)$$

For $h \approx 0$, eq. (5) may be rearranged (with $\gamma = v/h$ and $c_{th} = k_{th}/\rho c_v$) to be a boundary condition

$$\left.\frac{\partial T}{\partial y}\right|_{y=0} = -\frac{\tau v}{2\rho c_v c_{th}}\,. \qquad (6)$$

Equation (6) is valid for times much longer than the diffusion time across the shear zone (that is, for $\Delta t \gg h^2/c_{th}$). This is the *planar shear zone approximation*. Away from the shear zone, there is no heat generation, so eq. (5) rearranges to

$$\frac{\partial T}{\partial t} = c_{th}\frac{\partial^2 T}{\partial y^2}\,. \qquad (7)$$

Pore pressure generation and transport:

$$\frac{\partial p}{\partial t} = c_{hyd}\frac{\partial^2 p}{\partial y^2} + \Lambda\frac{\partial T}{\partial t}\,. \qquad (8)$$

where the thermal coupling parameter Λ is given by

$$\Lambda = \frac{\lambda_f - \lambda_\phi}{\beta_f + \beta_\phi}\,. \qquad (9)$$

If the thermal and fluid transport properties are uniform—and the planar shear zone approximation holds—then the pore pressure and temperature rise on the fault are uniquely related through [*Rice*, 2006]

$$\Delta T(y=0) = \frac{1+\sqrt{c_{hyd}/c_{th}}}{\Lambda}\Delta p(y=0)\,. \qquad (10)$$

4. WHEN IS THERMAL PRESSURIZATION IMPORTANT?

The time derivative of frictional resistance (3) may be decomposed as

$$\frac{d\tau_{fric}}{dt} = \underbrace{\frac{d\mu}{dt}(\sigma - p_0)}_{\text{friction}} - \underbrace{\mu_0\frac{dp}{dt}}_{\text{thermal pressurization}}\,. \qquad (11)$$

We define the critical velocity v_{crit} to be when the thermal pressurization term in eq. (11) is larger than the rate- and state-dependent friction term.

5. RESULTS — A. Aging law

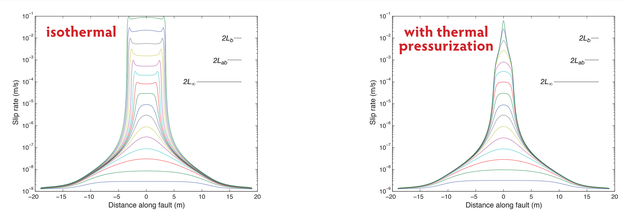

Figure 2. Results from aging law simulations in the isothermal (left) and thermal pressurization (right) cases. In these simulations, $a/b = 0.8$, $d_c = 100$ μm, and $(\sigma - p_0) = 140$ MPa. Lines represent snapshots taken at times corresponding to half-decade increases in maximum slip speed vmax from $10^{-9.5}$ m/s to 10^{-1} m/s. Scale bars show L_b [*Dieterich*, 1992], $L_{ab} = Gd_c/(b-a)\sigma_{eff}$, and L_∞ [*Ampuero & Rubin*, 2008].

At early times (low slip speeds) the two profiles are similar. At ~10^{-5} m/s, the profiles start to diverge. By ~10^{-4} m/s, the profiles have distinctly different forms.

At high slip speeds, the nucleation zone effectively shrinks to a point. This behavior is likely nonphysical and is either a consequence of (1) the numerical system failing to be well-posed (see fig. 3) or (2) the omission of an important physical process.

Figure 3. Identifying critical velocity. We show the weakening rates as decomposed in eq. (11) for the fastest-slipping point on the fault. The intersection of the two lines defines v_{crit}. The dotted line shows an analytical estimate of *Segall & Rice* [2006].

Color coded background indicates the validity of the planar shear zone approximation.

Yellow: $100h^2/c_{th} > \Delta t > 10h^2/c_{th}$ (probably OK)
Orange: $10h^2/c_{th} > \Delta t > h^2/c_{th}$ (questionable)
Red: $h^2/c_{th} > \Delta t$ (doubtful)

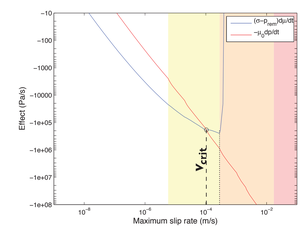

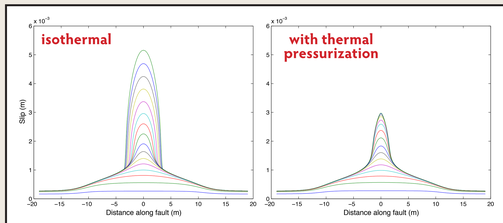

Figure 4. Additional aging law results. Snapshots correspond to those of fig. 2.

Far left— Cumulative slip during isothermal nucleation.

Near left— Cumulative slip during nucleation with thermal pressurization.

Right—Frictional stress profiles show the nucleation zone is not crack-like (that is, constant stress inside the zone), unlike isothermal aging law nucleation.

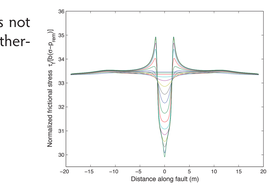

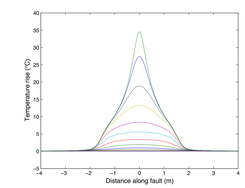

Left—Temperature rise resulting from shear heating. A modest rise in temperature yields significant weakening. Critical velocity v_{crit} corresponds to ~3°C of heating.

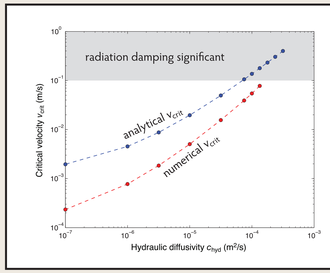

Figure 5. Critical velocity v_{crit} increases with hydraulic diffusivity c_{hyd}, holding all other parameters constant. An analytical estimate [Segall & Rice, 2006] is shown. Unlike the analytical estimate, the numerical v_{crit} reflects the heating-weakening-slip feedback cycle.

B. Slip law

Figure 6. Profiles of slip speed for slip law nucleation with thermal pressurization. Parameters are the same as for figs. 2-4, but we used the slip evolution law.

Isothermal slip law nucleation takes the form of a unidirectional slip pulse, but under some conditions, thermal pressurization prevents that from occurring.

Cumulative slip, temperature rise, and frictional stress are qualitatively similar for thermal pressurization under the slip law and aging law.

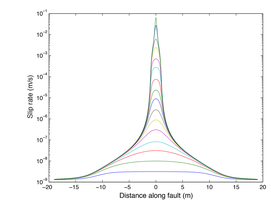

6. THE NEXT STEPS

The shrinking nucleation zone must be resolved. We know the problem to be poorly posed at high slip speeds (fig. 3), so we must abandon the planar shear zone approximation. Preliminary simulations suggest that doing so results in a nucleation zone that still shrinks, but does not become a slip "singularity."

The effect of varying effective normal stress on friction [*Linker & Dieterich*, 1992] is one additional mechanism that may reduce the "runaway" weakening resulting from thermal pressurization.

Looking ahead, we will conduct simulations that include both thermal pressurization and dilatant strengthening (see *Segall & others* poster, this conference). Such simulations will allow us to explore the competition between the two effects during nucleation, which may control whether slip ultimately becomes fast or slow.